Jitter Estimation and Mitigation in Sub-Nyquist Sampling using Slepian Functions

Hasan Basri Çelebi[†*] and Lütfiye Durak-Ata[‡]

[†] TÜBİTAK-BİLGEM, Kocaeli, Turkey
[*] Yıldız Technical University, Electronics and Communication Eng., Istanbul, Turkey
[‡] Istanbul Technical University, Institude of Informatics, Istanbul, Turkey
hasan.celebi@tubitak.gov.tr, lutfiye@ieee.org

Abstract

Impairments caused by timing jitter are one of the most important performance limiting factors of digital converters while sampling under Nyquist rates. In this paper, the effect of jitter in such cases is shown and a new method to estimate and reconstruct the timing jitter errors is presented. The system model is based on the estimation of jitter times with an annihilating filter and reconstruction of the signal using Slepian functions without the knowledge of input frequencies. It is shown that, a significant improvement on SNR is achieved.

1. Introduction

One of the key parameters that digital converters need to comply with is jitter, caused by imperfections of sampling clock of the analog to digital converter (ADC) [1]. Moreover, when it comes to sub-Nyquist sampling, which recently has been attracting more attention due to the discovery of new sampling techniques such as compressed sampling, the sampling block may become unusable due to jitter. Although, jitter reconstruction for Nyquist sampled band-limited signals is a well-studied topic in the literature [1, 2, 3, 4, 5], there are limited studies for jitter analysis and mitigation for sub-Nyquist sampled signals [6].

A straightforward linear time variant implementation method is proposed in [2]. However, due to the constraints set to the jitter values, it is suitable for practical applications. A jitter compensation system model has been proposed in [3] in which to estimate the jittered sampling instants, a clean reference tone is added to the incoming signal before sampling circuitry. This work has been focused on narrowband Nyquist sampled signals. A jitter tracking algorithm is proposed in [4] which uses the spectral characteristics of jitter. Instead adding a reference tone, a modulated high-frequency reference signal is injected to the received signal in[5]. It is shown that the proposed method is applicable even for wide-band signals. Jittered sub-Nyquist sampling is studied in [6]. A reference tone, similar to [3], is added to the sub-sampled signal before conversion. It is assumed that the sub-sampled incoming signal is a narrowband signal and the reference tone is located into low-frequency zone where the reference tone is sufficiently separated from the incoming signal. However, method proposed in [6] is not applicable for sub-Nyquist sampled wide-band signals.

In this paper, a novel jitter estimation and signal reconstruction method is presented for jittered sub-Nyquist sampled signals. Effects of jitter in sub-Nyquist sampled signals is analyzed and mathematical relation between Nyquist sampled and sub-Nyquist sampled signals is derived. The proposed system model is investigated deeply and compared with the other methods in the literature. It is shown that the proposed model is capable of estimating and mitigating the sampling jitter without any initial information, except the signal sub-band number and sampling frequency. The proposed model is based on detecting the sampling instants with an annihilating filter, then carrying the jittered sub-Nyquist sampled signal to base-band and mitigating the jitter by using Slepian functions.

2. Jitter analysis

Consider a real and continuous time sine-wave

$$x(t) = A\sin(2\pi f_i t + \theta) \tag{1}$$

with amplitude of A, frequency f_i, and phase angle θ. If the signal is sampled with a sampling rate of $f_s = 1/T_s$, the uniform sampling instants will be $t_n = nT_s$, $n \in \mathbb{Z}$. However, in some cases due to timing jitter effects sampling instants may be shifted over time as

$$\tau_n = nT_s + j_n, n \in \mathbb{Z} \tag{2}$$

where j_n is the timing jitter associated with the nth sample and modeled as a real valued random process with Loretzian shaped spectrum, having zero mean and variance σ^2 [5]. Let us denote the jitter error as

$$\xi(n) = x(nT_s) - x(nT_s + j_n). \tag{3}$$

It is clear that $\xi(n)$ represents the voltage difference caused by the jitter in j_n seconds, and approximated to the derivative of the signal as [1]

$$\xi(n) = j_n \frac{\partial x(\tau_n)}{\partial \tau_n}. \tag{4}$$

In order to show the effect of jitter error on signal to noise ratio (SNR), root mean square (RMS) value of $\xi(n)$ is calculated as

$$\mathcal{R}[\xi(n)] = j_r \mathcal{R}\Big[\frac{\partial x(t_n)}{\partial t_n}\Big] \tag{5}$$

where $\mathcal{R}[\cdot]$ is the RMS operator and j_r is the RMS jitter value. Hence the RMS jitter of $x(t)$ is $\mathcal{R}[\xi(n)] = j_r\sqrt{2}\pi f_i A$. It is straightforward to calculate the SNR of a jittered sampled sine-wave as

$$\text{SNR}(dB) = -20\ \log(j_r 2\pi f_i) \tag{6}$$

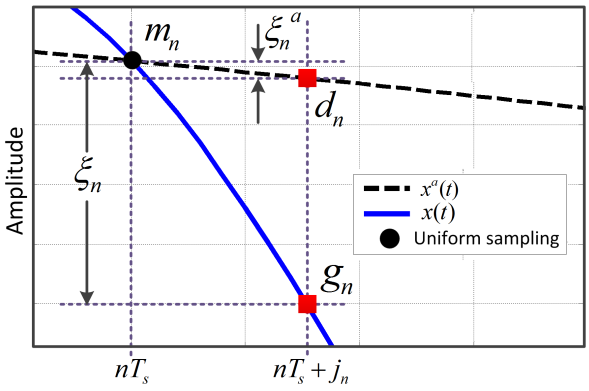

Figure 1. Jitter error comparison between ξ_n and ξ_n^a, where g_n and m_n are the samples of $x(t)$ with and without jitter, respectively, and d_n is the jittered sample where the input signal is $x^a(t)$

3. Jittered sub-Nyquist sampling

In some applications, the input analog signal is sampled under Nyquist rate such as, direct IF sampling, compressed sampling or multi-coset sampling. Input signal frequency is larger than half of sampling frequency $f_i > f_s/2$ in these type of cases. Sampling the signal with f_s in such a scenario will shift the signal to the baseband due to the aliasing effect where the relationship between the input frequency f_i and aliased frequency f_i^a is

$$f_i = \kappa f_s + f_i^a, \quad f_i^a < f_s/2, \tag{7}$$

κ is the number of the sub-band where the input signal is located.

In order to analyze jitter error on sub-Nyquist sampling, relation between f_i and SNR needs to be revealed. For simplicity, let us denote the jittered clock as a sine-wave of frequency f_s. RMS of clock phase noise ϕ_r is related to the jitter timing as $\phi_r = 2\pi f_s j_r$. Now it is possible to express the SNR value as a function of ADC clock frequency and input signal frequency.

$$\text{SNR}(dB) = -20 \log\left(\phi_r \frac{f_i}{f_s}\right) \tag{8}$$

By analyzing (4) and (8), the same amount of timing jitter causes much more jitter error while sampling sub-Nyquist rate. An example is depicted in Fig.1, where the aliased signal is represented as

$$x_a(t) = A\sin(2\pi f_i^a t + \theta) \tag{9}$$

and g_n, d_n, and m_n stand for the jittered samples of $x(t)$, jittered samples as if the input signal was $x_a(t)$, and the jitterless uniform samples, respectively. Due to the rapid changes in $x(t)$, jitter error increases $\xi_n > \xi_n^a$ when input frequency increases.

To show the SNR degradation caused by jitter error while sub-Nyquist sampling for different input frequencies simulation and theoretical results are plotted in Fig.2, where the input signal is $x(t) = \sin(2\pi f_i \tau_n)$ and $f_i = f_i^a + \kappa f_s$ for $f_s = 100$MHz, $f_i^a = 10$MHz, and $j_r = 10, 25, 50, 100$ps. It is shown that, increase in input frequency f_i results in rapid decrease on SNR. Even a small jitter may cause the ADC block unusable for sub-Nyquist sampling cases. Note that, these amount of jitter RMS values are largely within ADCs tolerance range.

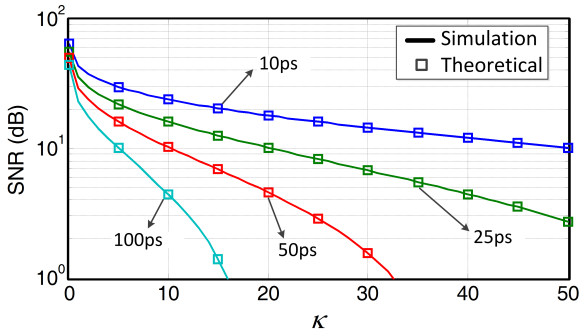

Figure 2. SNR degradation due to sampling clock jitter vs κ values where κ is the sub-band number of the input signal frequency $f_i = \kappa f_s + f_i^a$, $f_i^a < f_s/2$

4. Reconstruction

The goal of jitter reconstruction is to reach the jitterless samples m_n. The starting point for jittered Nyquist rate sampled signals is d_n, however, when it comes to jittered sub-Nyquist sampling, g_n is the input. The proposed reconstruction method has two steps. Goal of the first step is to convey the jittered samples g_n, to baseband jittered samples d_n^*. Second step is the jitter reconstruction to reach jitterless samples m_n^*. No initial information is assumed to be known, except κ and f_s. The proposed system model has been shown in Fig.3. The main contribution of this study is the proposed system for jitter estimation and signal reconstruction. As seen in Fig.3 instead of a single branch of sampling, two coherent sampling lines added to transfer the jittered samples to baseband and reconstruct the jitter. Although additional sampling branches increase the complexity of the sampling block, the total SNR improvement achieved after reconstruction can be more than 25dB.

4.1. Single sine-wave

Let us start with a single sine-wave signal $x(t)$ of frequency f_i and amplitude A. Sub-sampling $x(t)$ with f_s where $f_i = \kappa f_s + f_a$ for $f_a < f_s/2$ will lead to get the same samples while sampling $x^a(t) = A\sin(2\pi f_a t)$ with f_s. These samples can be expressed as m_n

$$m_n = A\sin(2\pi f_a n T_s), \quad n \in \mathbb{Z} \tag{10}$$

Due to timing jitter g_n will be

$$g_n = A\sin(2\pi f_i \tau_n), \quad n \in \mathbb{Z} \tag{11}$$

while d_n can be expressed as

$$\begin{aligned} d_n &= A\sin(2\pi f_a \tau_n) \\ &= A\sin\left(2\pi(f_i - \kappa f_s)\tau_n\right), \quad n \in \mathbb{Z} \end{aligned} \tag{12}$$

Solving d_n by using trigonometric identities, one will get

$$d_n = g_n \cos(2\pi\kappa f_s \tau_n) - h_n \sin(2\pi\kappa f_s \tau_n) \tag{13}$$

where $h_n = \alpha_n\sqrt{\Psi_n - g_n^2}$ for $\Psi_n = A^2$ and $\alpha_n = \pm 1$ which is related to the slope of $x(t)$ at τ_n.

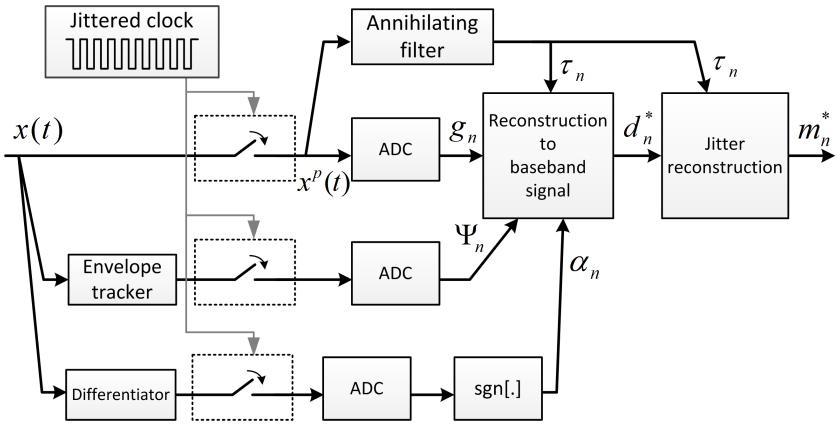

Figure 3. The proposed system model

4.2. Two sine-waves

If the input signal $x(t)$ is sum of two sine-waves

$$x(t) = A_1 \sin(2\pi f_1 t) + A_2 \sin(2\pi f_2 t) \tag{14}$$

where $f_1 = \kappa f_s + f_1^a$ and $f_2 = \kappa f_s + f_2^a$, for $f_1^a < f_s/2$, $f_2^a < f_s/2$, jitterless samples m_n and jittered sampled samples g_n and d_n can be expressed as

$$m_n = A_1 \sin(2\pi f_1 n T_s) + A_2 \sin(2\pi f_2 n T_s) \tag{15}$$
$$g_n = A_1 \sin(2\pi f_1 \tau_n) + A_2 \sin(2\pi f_2 \tau_n) \tag{16}$$
$$d_n = A_1 \sin(2\pi f_1^a \tau_n) + A_2 \sin(2\pi f_2^a \tau_n). \tag{17}$$

By solving d_n according to $f_1^a = f_1 - \kappa f_s$ and $f_2^a = f_2 - \kappa f_s$, one will get

$$d_n = g_n \cos(2\pi\kappa f_s \tau_n) - h_n \sin(2\pi\kappa f_s \tau_n) \tag{18}$$

where

$$h_n = \alpha_n \sqrt{\Psi_n - g_n^2} \tag{19}$$

and

$$\Psi_n = A_1^2 + A_2^2 + 2A_1A_2 \cos\big(2\pi(f_1^a - f_2^a)\tau_n\big). \tag{20}$$

4.3. Multiple sine-waves

Let us represent $x(t)$ as the sum of M sine-waves

$$x(t) = \sum_{k=1}^{M} A_k \sin(2\pi f_k t) \tag{21}$$

where input frequencies are larger than f_s but located in the same sub-band κ. Passing directly to the relation between d_n and g_n one will find that

$$d_n = g_n \cos(2\pi\kappa f_s \tau_n) - h_n \sin(2\pi\kappa f_s \tau_n) \tag{22}$$

where

$$h_n = \alpha_n \sqrt{\Psi_n - g_n^2} \tag{23}$$

and

$$\Psi_n = \sum_{i=1}^{M-1} \sum_{j=i+1}^{M} A_i^2 + 2A_iA_j \cos\big(2\pi(f_i - f_j)\tau_n\big). \tag{24}$$

4.4. Proposed system model

It is clear that the relationship between g_n and d_n is related to the jittered sampling instants τ_n, κ, and h_n. Having a closer look at Ψ_n and α_n, one will see that Ψ_n is the square of the envelope of $x(t)$

$$\Psi = z\big[x(t)\big]^2 \tag{25}$$

where $z[\cdot]$ represents the envelope of the signal and α_n depends on the slope of $x(t)$ at jittered sampling times τ_n and can be expressed as

$$\alpha_n = \text{sgn}[\partial x(\tau_n)/\partial\tau_n] \tag{26}$$

where sgn$[\cdot]$ is the signum function. In order to estimate Ψ_n and α_n at jittered sampling instants, two additional sampling branches, which use the same clock with the main sampling branch, are added as shown in Fig.3. Consequently, with the estimation of jittered sampling times τ_n, reconstruction to d_n become possible.

4.5. Estimation of sampling instants

Sampling can be modeled by use of periodic impulse train. Signal after a jittered impulse-train sampler becomes a stream of diracs

$$x^p(t) = \sum_{n\in Z} x(\tau_n)\delta(t - \tau_n). \tag{27}$$

By considering the periodic extension of stream of dirac functions, the signal can be represented as

$$x^p(t) = \sum_{k=-\infty}^{\infty} X_k e^{2ik\pi t/T_s} \tag{28}$$

where the Fourier coefficients are

$$X_k = \sum_{n=1}^{N} x(\tau_n) e^{-2ik\pi\tau_n/T_s}, \tag{29}$$

linear combination of N exponentials.

Consider convolving X_k with an annihilating filter having N zeros at

$$u_n = e^{-2i\pi\tau_n/T_s} \tag{30}$$

that is [7]

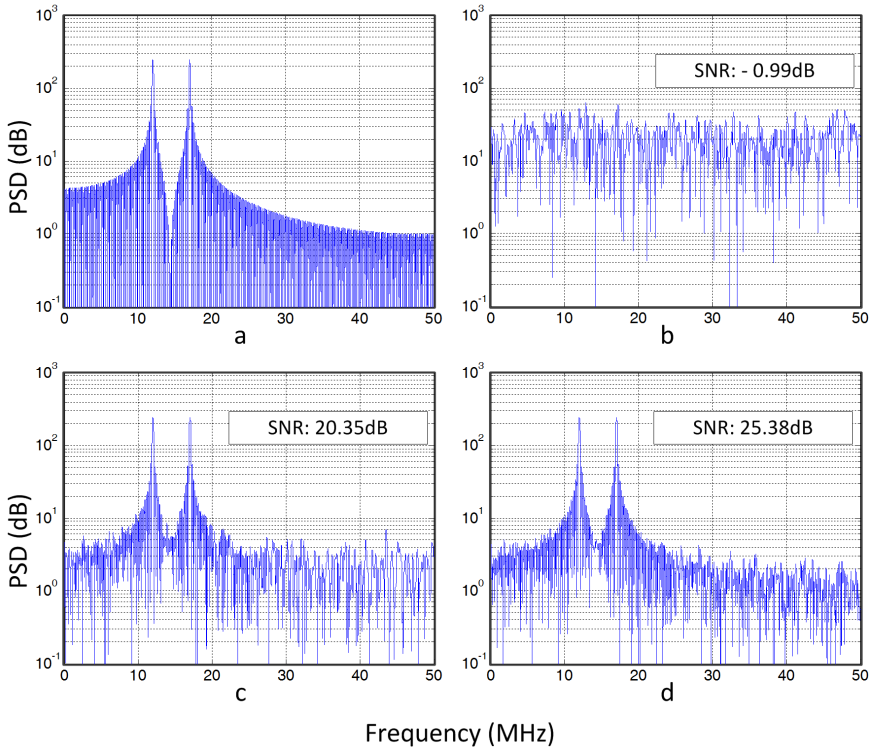

Figure 4. PSD of a-jitterless sub-sampled $x(t)$, b-jittered sub-sampled $x(t)$, c-output of the first reconstruction step, d-reconstructed signal

$$A(z) = \prod_{n=1}^{N}(1 - u_n z^{-1}) = \sum_{n=0}^{N} \varphi_n z^{-n}. \tag{31}$$

Each exponential of X_k will be zeroed out by the roots of φ_n. The problem then becomes to find the roots that match X_k.

$$\sum_{n=0}^{N} \varphi_n X_{k-n} = \sum_{n=0}^{N}\sum_{m=1}^{N} x(\tau_m) u_m^{k-n} \varphi_n \tag{32}$$

$$= \sum_{m=1}^{N} x(\tau_m) u_m^{k} \sum_{n=0}^{N} \varphi_n u_m^{-n} = 0 \tag{33}$$

Zeros of $A(z)$ uniquely define τ_n. Solving the above equation is related to Prony's method [7].

4.6. Jitter mitigation

A band-limited signal $s(t)$ is uniquely represented by its samples by

$$s(t) = \sum_{n\in\mathbb{Z}} s(nT_s)\text{sinc}(t - nT_s) \tag{34}$$

where

$$\text{sinc}(t - nT_s) = \frac{\sin\left(\pi(t - nT_s)\right)}{\pi(t - nT_s)}, -\infty < t < \infty \tag{35}$$

is the orthogonal basis function. However, for time-limited signals sinc$(\cdot)$ may not the best kernel function, since significant part of the energy lies out of the time limit of $s(t)$, which causes reconstruction errors. Among all the orthogonal basis functions defined in a limited time, Slepian functions have the highest energy concentration in a limited band, and vice versa. Slepian functions are the solution of the problem of concentrating a bandlimited signal into a time interval.

$$p(t) = \frac{1}{2\pi}\int_{-W}^{+W} P(\omega) e^{i\omega t} d\omega \tag{36}$$

where $p(t)$ represents Slepian function and W is the bandwidth of the $p(t)$. Slepian functions optimize the concentration of time-frequency uncertainty principle. They are eigenfunctions of a kernel that depends on the time-frequency product TW.

$$\int \Big[\frac{\sin TW(t - t')}{\pi(t - t')}\Big] p(t')dx' = \lambda p(t) \tag{37}$$

where

$$\lambda = \frac{\int_{-T}^{+T} g^2(t)dt}{\int_{-\infty}^{+\infty} g^2(t)dt} \tag{38}$$

Due to the spectral efficiency reasons, Slepian functions are considered through the jitter reconstruction process. Jittered sampled signal reconstruction procedure by Slepian functions is deeply analyzed in [8]. We refer [8] and its references for further information.

5. Simulations

In this section, the performance of the proposed method is demonstrated by applying it to a jittered sub-Nyquist sampled signal

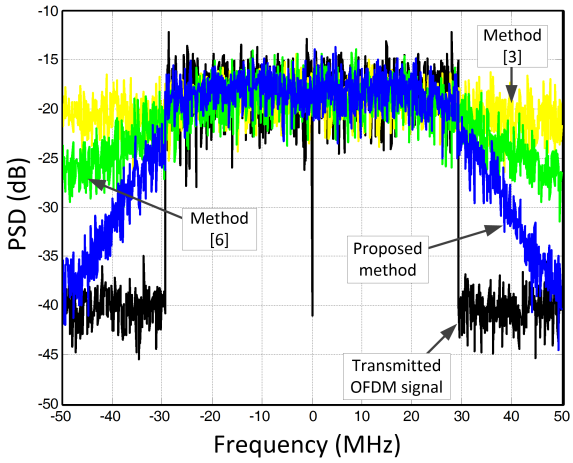

Figure 5. Transmitted OFDM signal and jitter mitigation performance of the proposed model and other methods from [3] and [6] when 150ps RMS jitter is applied to the sub-sampled signal.

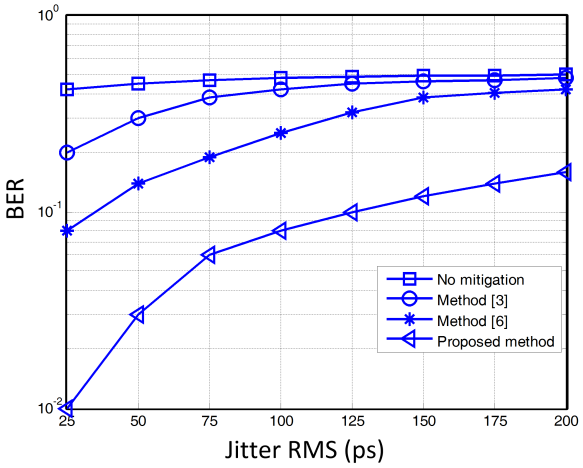

Figure 6. BER results of the proposed method and methods from [3] and [6] are compared for different jitter RMS values.

$$x(t) = \sum_{i=1}^{2} A_i \sin(2\pi f_i t) \tag{39}$$

where $f_1 = 1012$MHz, $f_2 = 1017$MHz, and $f_s = 100$MHz. 1ns of RMS jitter value is introduced to sampling clock. Power spectral densities (PSD) of the results are shown in Fig.4. PSD of jitterless sub-sampled $x(t)$ can be seen in Fig.4-a. Note that no noise is introduced to the input signal. Jittered sub-sampling demolishes $x(t)$, as shown in Fig.4-b where SNR drops to -1dB. After the first step of the proposed method, SNR of the reconstructed signal d_n^* is calculated as 20.35dB, which is $\sim$ 21dB of improvement. After the second step, SNR increases to 25.38dB which concludes a total 26dB of SNR improvement. Note that, the performance of the proposed method is directly related to the performance of the annihilating filter.

In order to see the effectiveness of the proposed system model, a simulation environment consists of a wide-band OFDM signal with 1024 subcarriers transmitted at 2.4GHz is deployed. Sampling frequency is set to 100MHz and SNR is 20dB. Jittered sub-Nyquist sampling is performed to the received signal with different jitter RMS values. The proposed jitter mitigation technique with two other methods presented in [3] and [6] are applied to the jittered samples. BER results are investigated while increasing the jitter RMS value from 25ps to 200ps, which can be accepted as one of the most challenging case. The transmitted OFDM signal can be seen in Fig. 5 with the output signals of three compared methods when 150ps RMS jitter is applied to the sub-sampled signal. BER results are depicted in Fig. 6. Performance of the proposed method outperforms the methods in [3] and [6]. It is natural, because both methods are developed for narrow-band signals. It is worth saying that, although jitter noise spectrum is assumed to be Loretzian shaped, the method proposed in this paper is not restricted to a specific type of jitter noise.

6. Conclusion

In this paper, effects of jitter on sub-Nyquist sampled signals are investigated and a complete jitter reconstruction system model for jittered sub-Nyquist sampled signals is presented. No initial information except the sampling rate and the sub-band of the input signal is needed. It is shown that more than 25dB of SNR improvement is achieved.

7. References

[1] Azeredo-Leme, C., "Clock Jitter Effects on Sampling: A Tutorial," IEEE Circuits and Systems Magazine, vol.11, no.3, pp.26,37, 2011

[2] Plotkin, E. I.; Roytman, L. M.; Swamy, M. N. S., "Reconstruction of nonuniformly sampled band-limited signals and jitter error reduction," Signal Processing, vol.7, pp.151-160, 1984

[3] Rutten, R.; Breems, L.J.; van Veldhoven, Robert H.M., "Digital jitter-cancellation for narrowband signals," IEEE International Symposium on Circuits and Systems, 2008

[4] Rabbi, M.F.; Ko, C.C., "Modeling, estimation and mitigation of colored timing jitter for OFDMA system," IEEE Consumer Communications and Networking Conference, 2012

[5] Liu, Y.; Pan, W.; Shao, S.; Tang, Y., "A new predistortion architecture with sampling clock jitter mitigation for wideband systems," IEEE Global Communications Conference, 2013

[6] Syrjala, V.; Valkama, M., "Sampling jitter estimation and mitigation in direct RF sub-sampling receiver architecture," IEEE 6th International Symposium on Wireless Communication Systems, 2009

[7] Vetterli, M.; Marziliano, P.; Blu, T., "Sampling signals with finite rate of innovation," IEEE Transactions on Signal Processing, vol.50, no.6, pp.1417-1428, 2002

[8] Senay, S.; Chaparro, L. F.; Durak, L., "Reconstruction of nonuniformly sampled time-limited signals using prolate spheroidal wave functions," Signal Processing, vol.89, pp.2585-2595, 2009